Electronic Supplementary Material (ESI) for Journal of Materials Chemistry C.

Supporting Information

Enhancing hydrogen generation through urea electro-oxidation on bimetallic and dual-anionic NiFeSP/NF nano-structured electrode

Shahab Paygozar[a], Alireza Sabour Rouhaghdam[a], Zhenyu Li[c], Taihuan Shao[c], Ghasem Barati Darband[b]*, Jinyang Li[c,d,e]*

a. Department of Materials Engineering, Faculty of Engineering, Tarbiat Modares University, P.O. Box: 14115-143, Tehran, Iran

b. Materials and Metallurgical Engineering Department, Faculty of Engineering, Ferdowsi University of Mashhad, Mashhad 91775-1111, Iran

c. School of Chemistry, Southwest Jiaotong University, Chengdu, 610031, China

d. Yibin Institute of Southwest Jiaotong University, Yibin 644000, China.

e. SWJTU-Leeds Joint School, Southwest Jiaotong University, Chengdu, 611756, China

Corresponding Author

*E-mail: baratidarband@um.ac.ir (Ghasem Barati Darband)

jinyang.li@swjtu.edu.cn (Jinyang Li)

Electrochemical measurements

Noteworthy, is the fact that each current density level was performed for 900 seconds. Hydrogen gas produced from an alkaline solution containing urea in a cell containing a couple of NiFeSP/NF||NiFeSP/NF was measured using gas chromatography at 50 mA.cm^{-2} current density according to i-t values every ten minutes; based on this, faradic efficiency is calculated as below:

$$FE_{H2} = \frac{2 \times 96485 \times nH2}{QHER} \quad (1)$$

$$n_{H2} = \frac{VH2}{Vm} \quad (2)$$

In relation to this matter, the overall charge distribution of the electrocatalyst is represented by Q, while the gas volume obtained from gas chromatography is denoted by V. The molar volume, which is equivalent to 22.4 L.mol^{-1}, is represented by Vm, and the molar mass of the gas produced is represented by n.

In addition, the potentials presented in this study were all investigated, employing the below equation which has been developed based on the reversible hydrogen electrode (RHE).

$$V_{RHE}=V(vs.Ag/AgCl)+ V° Ag/AgCl + 0.059 pH \quad (3)$$

To analyze electrochemical interfaces the double-layer capacitance (Cdl), roughness factor (RF), and electrochemical surface area (ECSA) can be calculated as follows;

To determine various electrodes' C_{dl}, CV curves were used. Accordingly, CV tests were conducted in the non-faradic potentials area (-0.74 to -0.84 V vs. Ag/AgCl) at scan rates ranging from 10 to 120 mV.s^{-1}. By utilizing the subtracting of current densities of cathode and anode (J_{anodic}-$J_{cathodic}$) employing various scan rates, values of C_{dl} were determined. The equation provided below was utilized to calculate the ECSA values:

$$ECSA= \frac{c_{dl}}{c_s} \quad (4)$$

Cs denotes the flat surface capacitance (20 µF.cm^{-2}). The RF value obtained by solving equation (5):

$$RF = \frac{C_{dl}}{C_0} \quad (5)$$

C_0 is used for the theoretical planar metal oxide capacitance, which is specifically representative of NiO with a surface smoothness of 60 µF.cm^{-2}.

Turnover frequency (TOF) Calculation

Equation (6) was used to calculate the turnover frequency (TOF) of HER at a fixed overpotential by considering the surface area of the geometric substrate and the current density. These TOF values were then used to generate graphs;

$$TOF = \frac{Total\ Hydrogen\ Turn\ Overs/cm^2\ geometric\ area}{Surface\ active\ sites/cm^2\ geometric\ area} \quad (6)$$

The total number of evolved hydrogen bubbles is calculated in accordance with the current density at a given overpotential on the basis of equation (7):

$$H_2 = \left(j\frac{mA}{cm^2}\right)\left(\frac{1C.s^{-1}}{1000\ mA}\right)\left(\frac{1\ mol.e^{-1}}{96485.3\ C}\right)\left(\frac{1\ mol.H_2}{2\ mol.e^-}\right) \times \left(\frac{6.022 \times 10^{23}\ H_2\ molecules}{1\ mol\ H_2}\right) = 3.12 \times 10^{15}\ \frac{\frac{H_2}{s}}{\frac{mA}{cm^2}}\ per \quad (7)$$

Supposing that all sites at the catalyst surfaces can participate as active centers for HER, their number is calculated as below:

$$N = \left(\frac{4\ atoms}{43.76\ A^{\circ}}\right)^{2/3} = 9.01 \times 10^{14}\ atoms.cm_{real}^{-2} \quad (8)$$

$$TOF = \frac{\left(3.12 \times 10^{15}\ \frac{\frac{H_2}{s}}{cm^2}\ per\ \frac{mA}{cm^2}\right) \times |j|}{\left(9.01 \times 10^{14} atoms.cm_{real}^{-2}\right) \times A_{ECSA}} \quad (9)$$

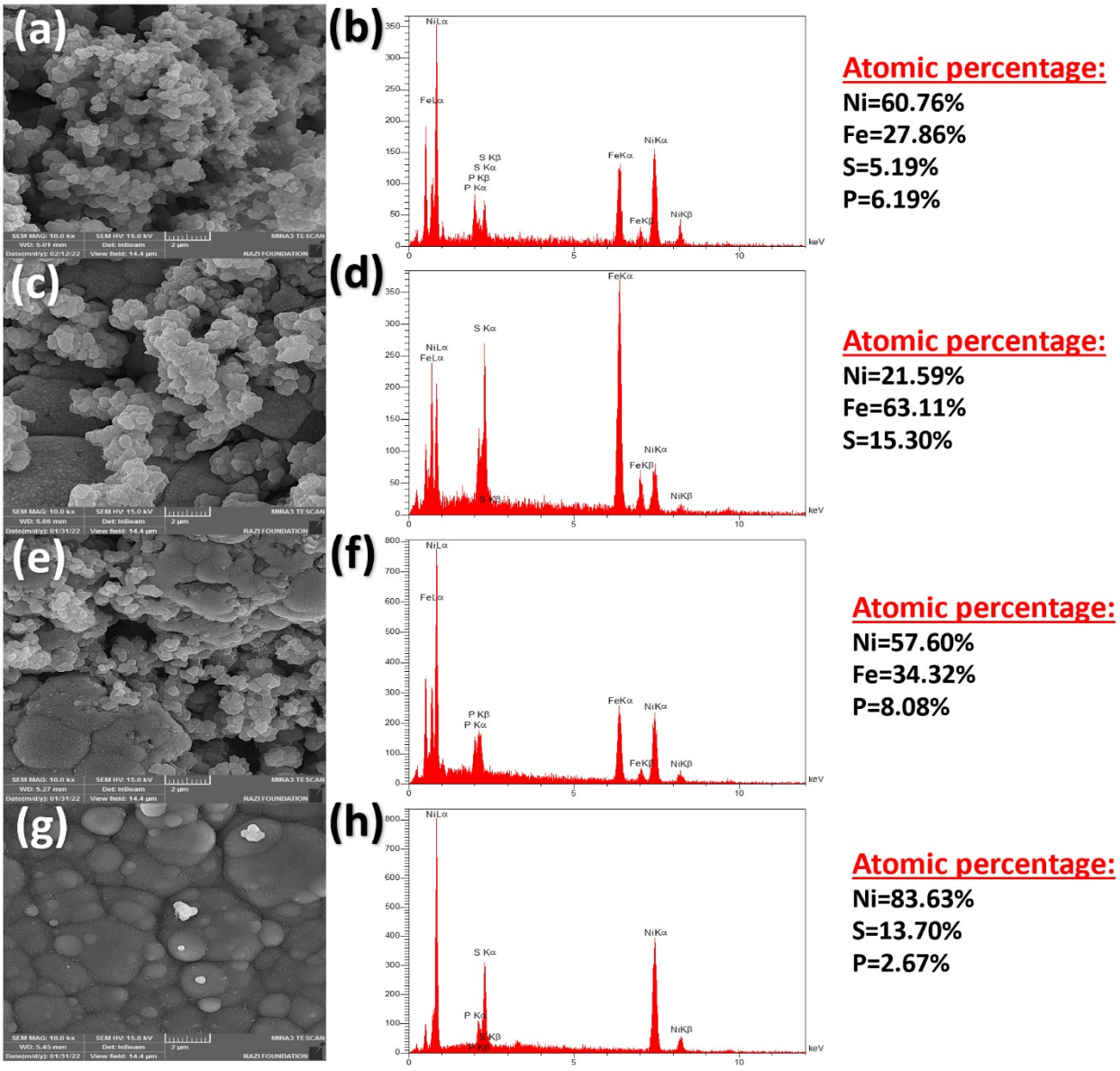

Figure S1 FE-SEM images and EDS spectra for prepared electrodes. (a, b) NiFeSP/NF. (c, d) NiFeS/NF. (e, f) NiFeP/NF. (g, h) NiSP/NF.

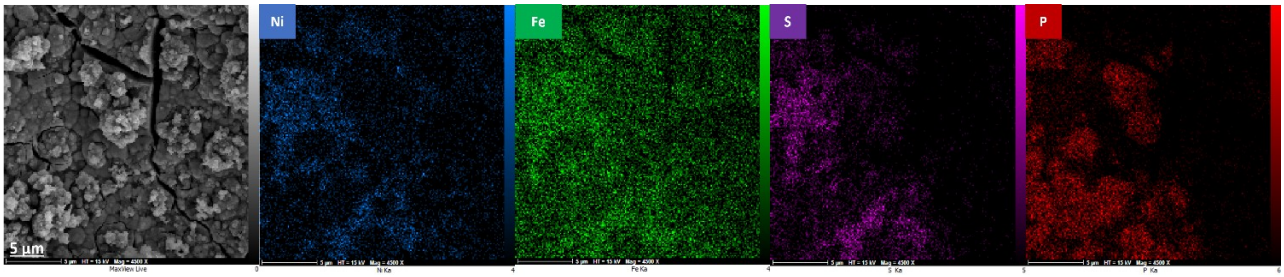

Figure S2 EDS-elemental mapping of NiFeSP electrode, Ni (blue), Fe (green), S (purple) and P (red).

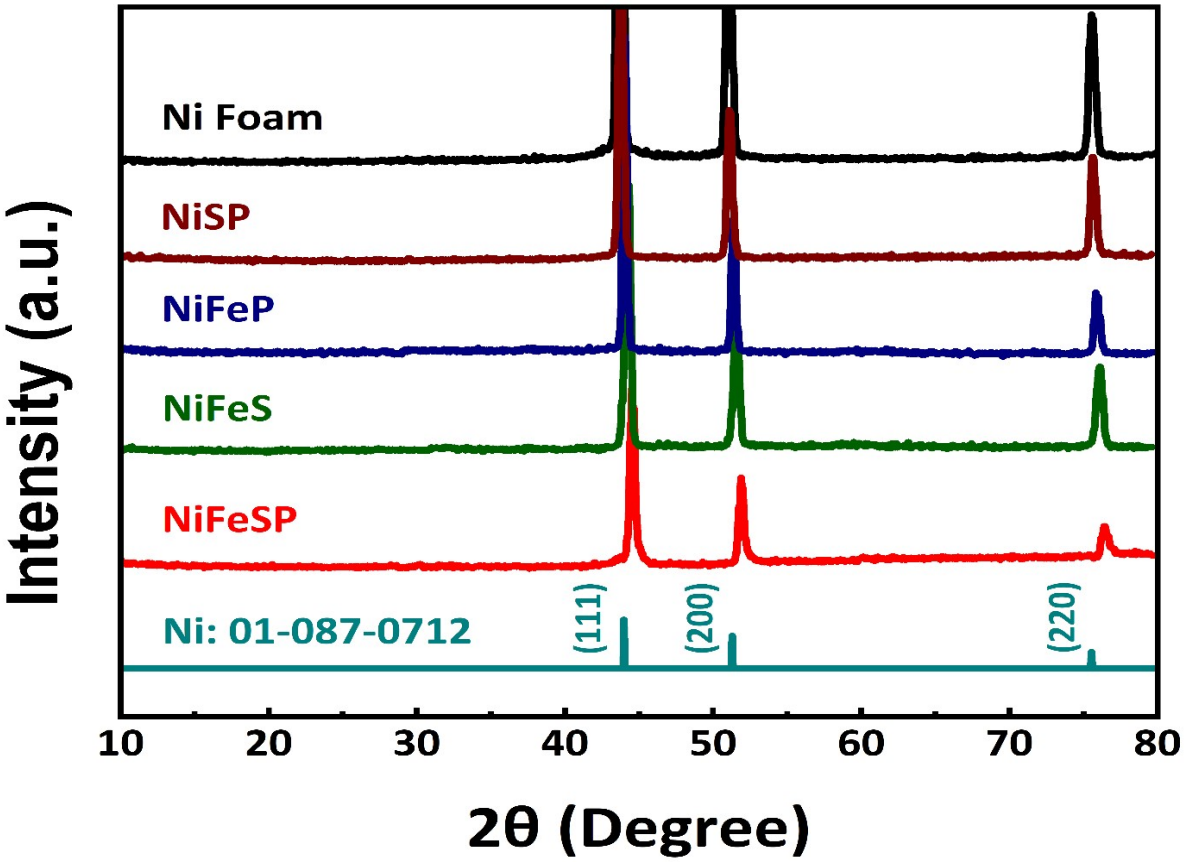

Figure S3 XRD pattern of Ni, NiFeSP, NiFeS, NiFeP and Ni foam.

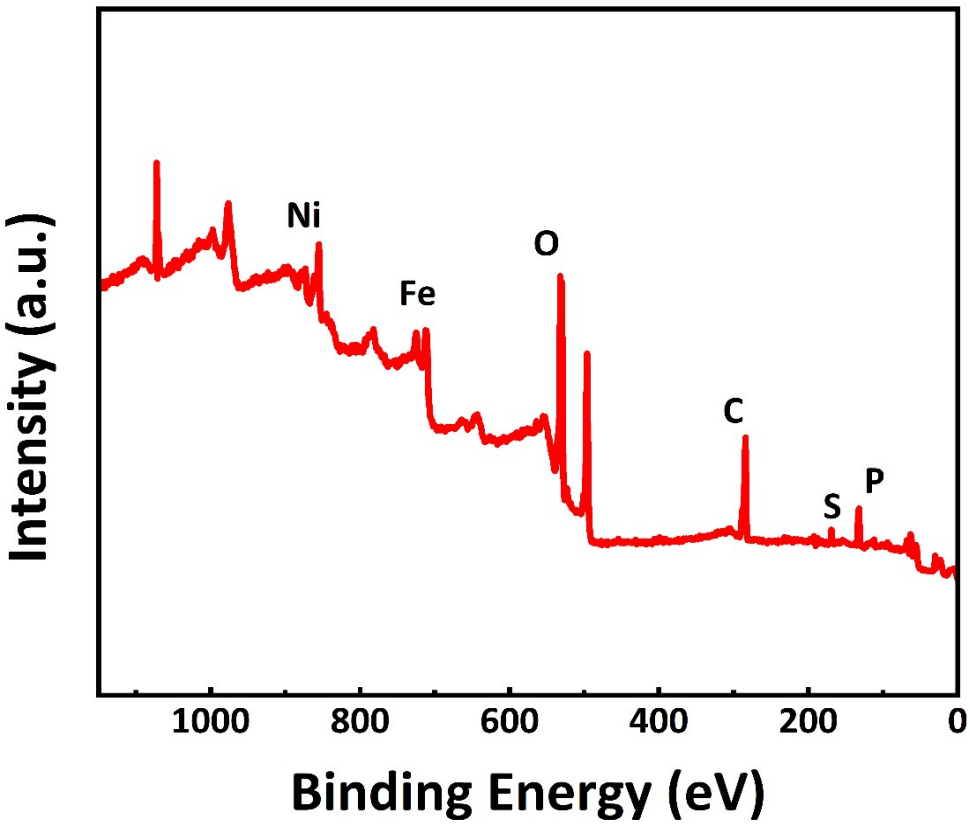

Figure S4 XPS survey spectra of NiFeSP electrocatalyst.

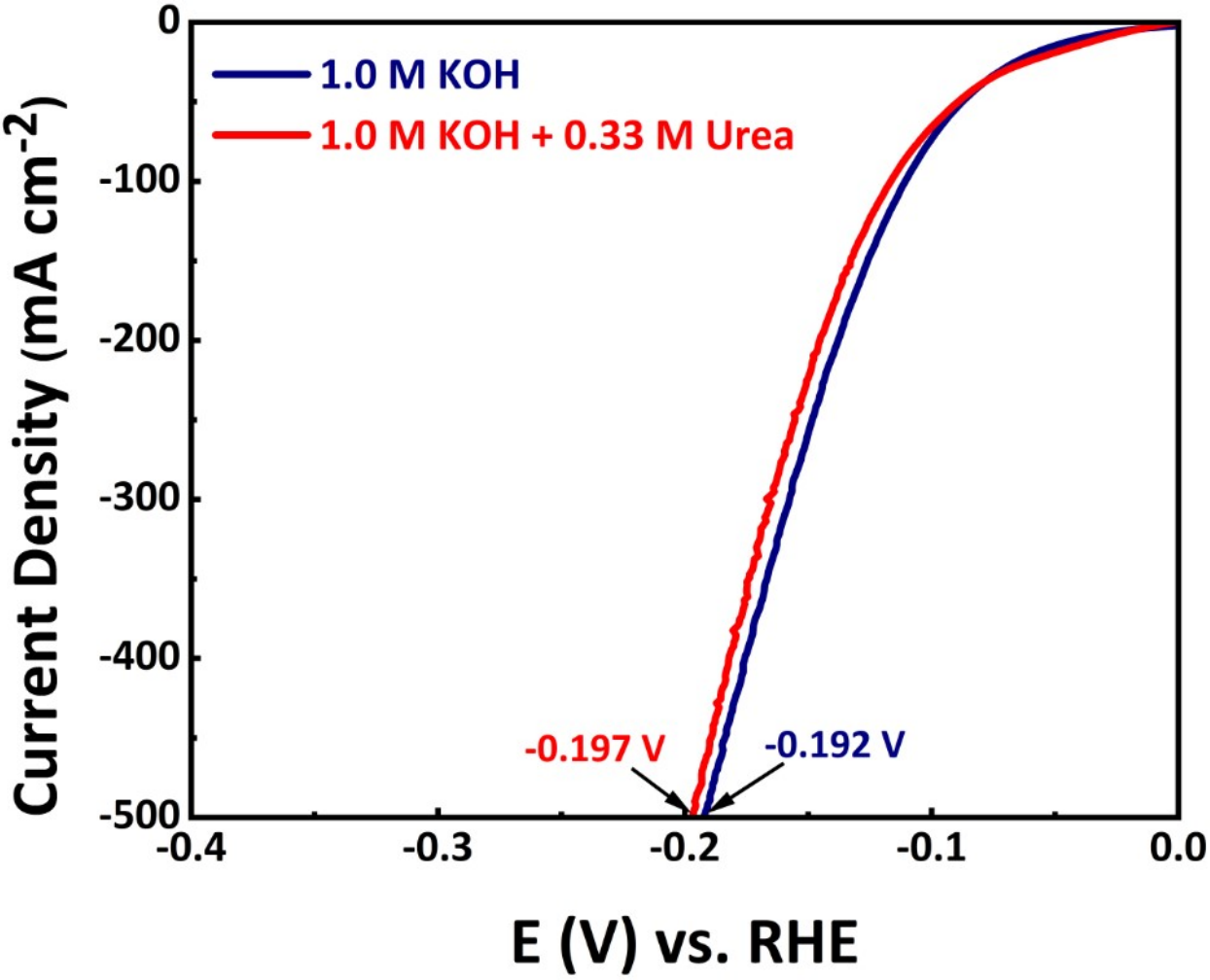

Figure S5 Polarization curves for the HER in 1000.0 mM KOH and 1000.0 mM KOH + 330.0 mM urea solutions.

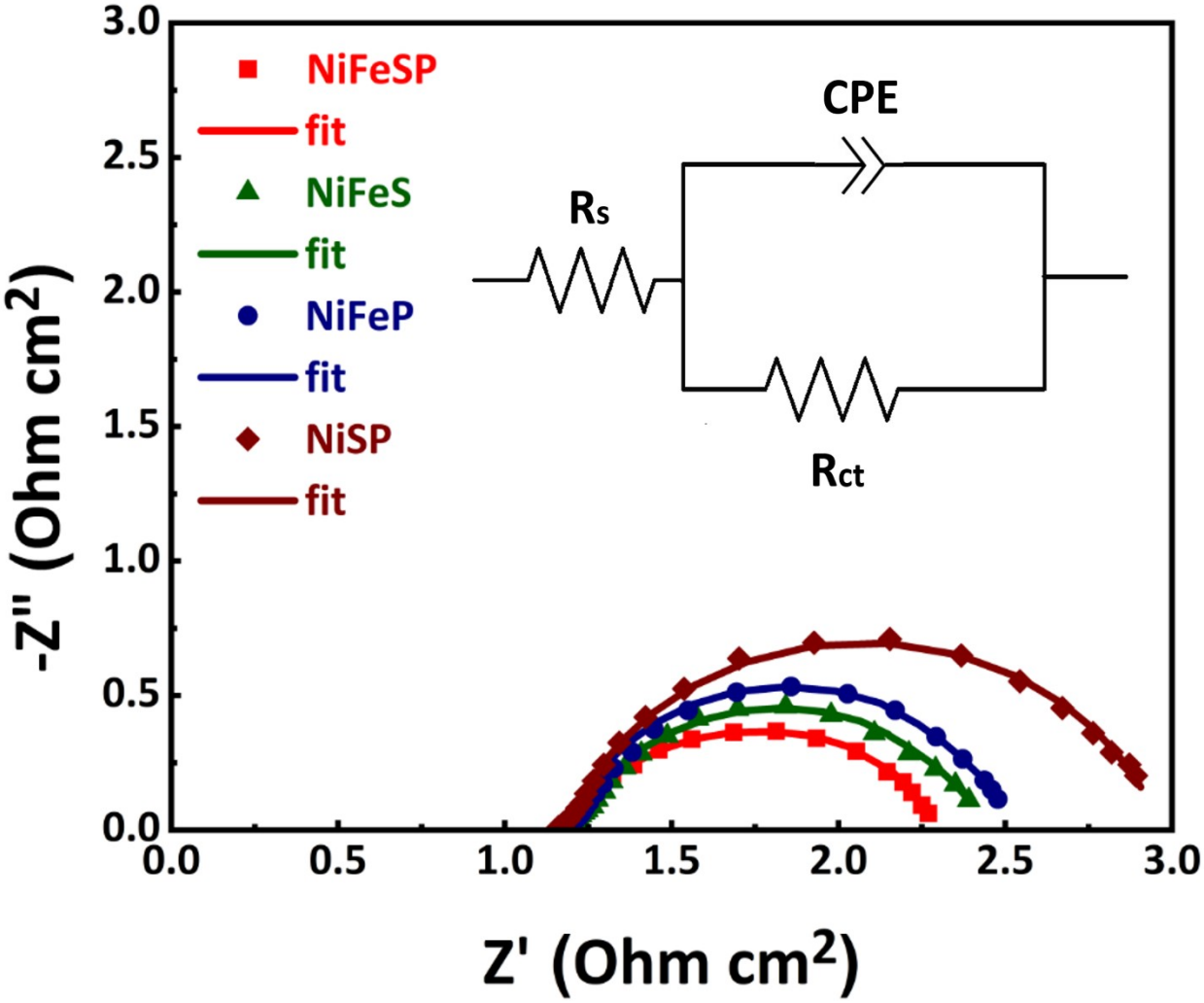

Figure S6 Nyquist curves of NiFeSP, NiFeS, NiFeP, and NiSP nanostructure in 1000.0 mM KOH.

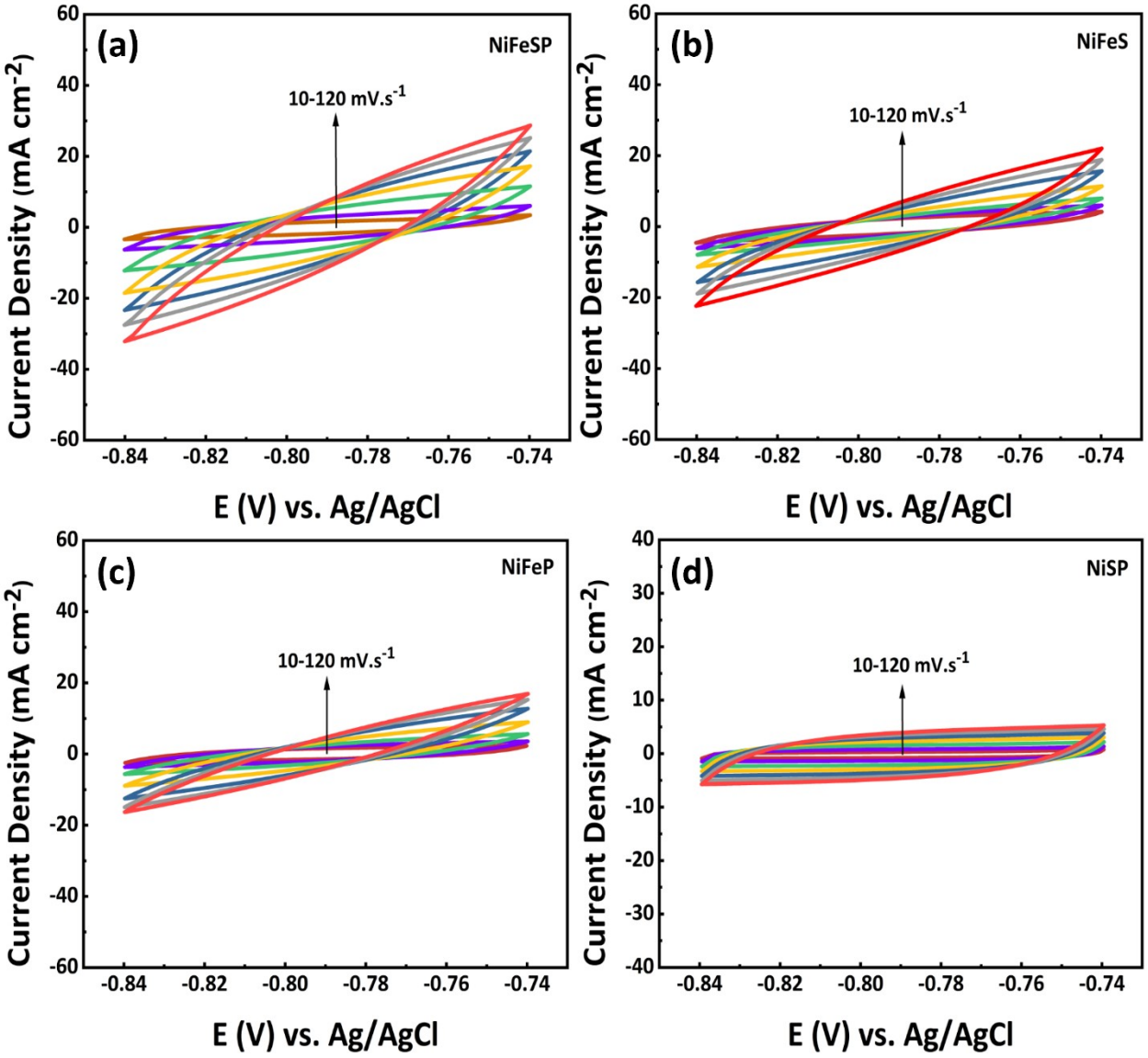

Figure S7 CV curves for (a) NiFeSP, (b) NiFeS, (c) NiFeP, and (d) NiSP electrocatalysts.

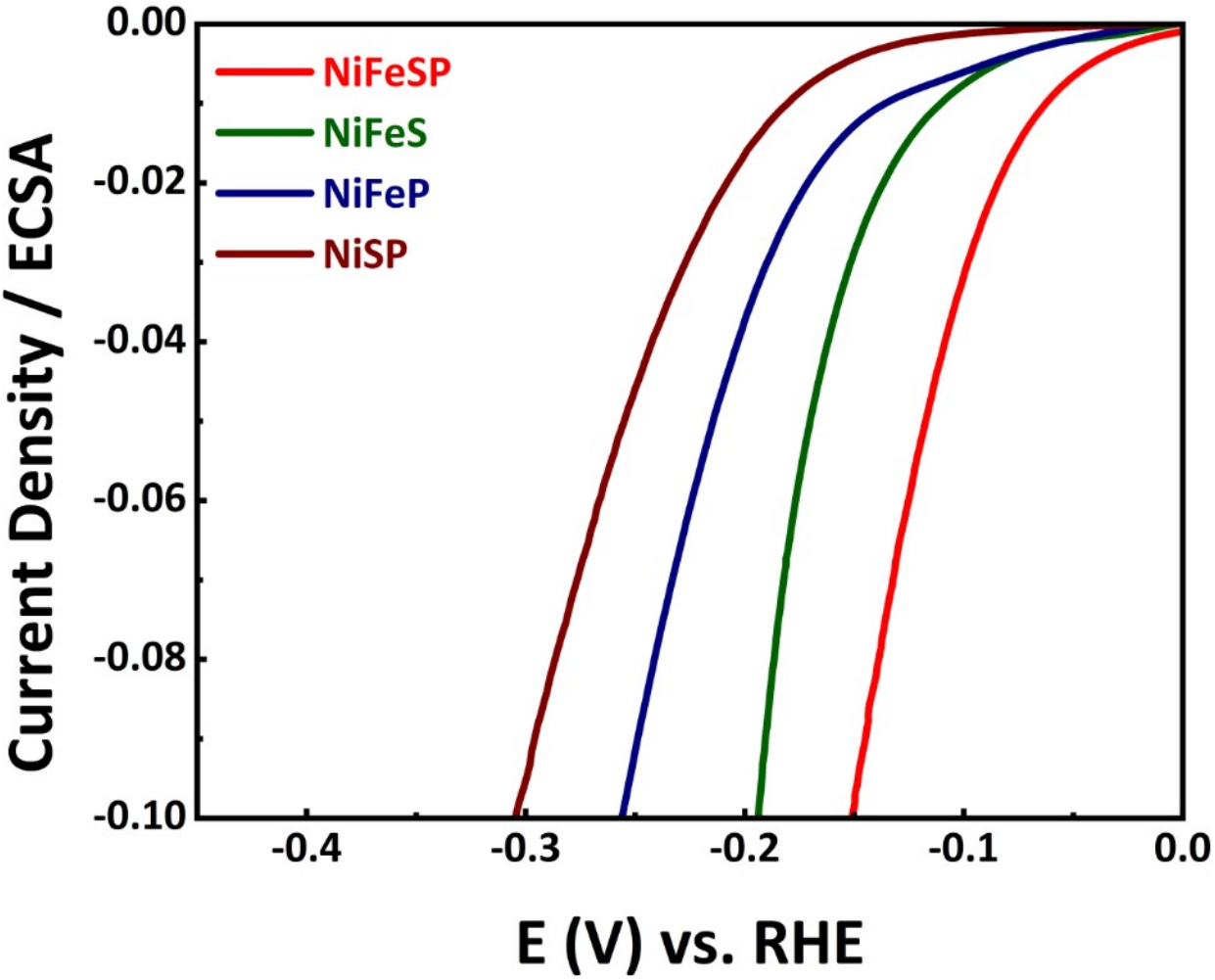

Figure S8 Normalized current densities to ECSA.

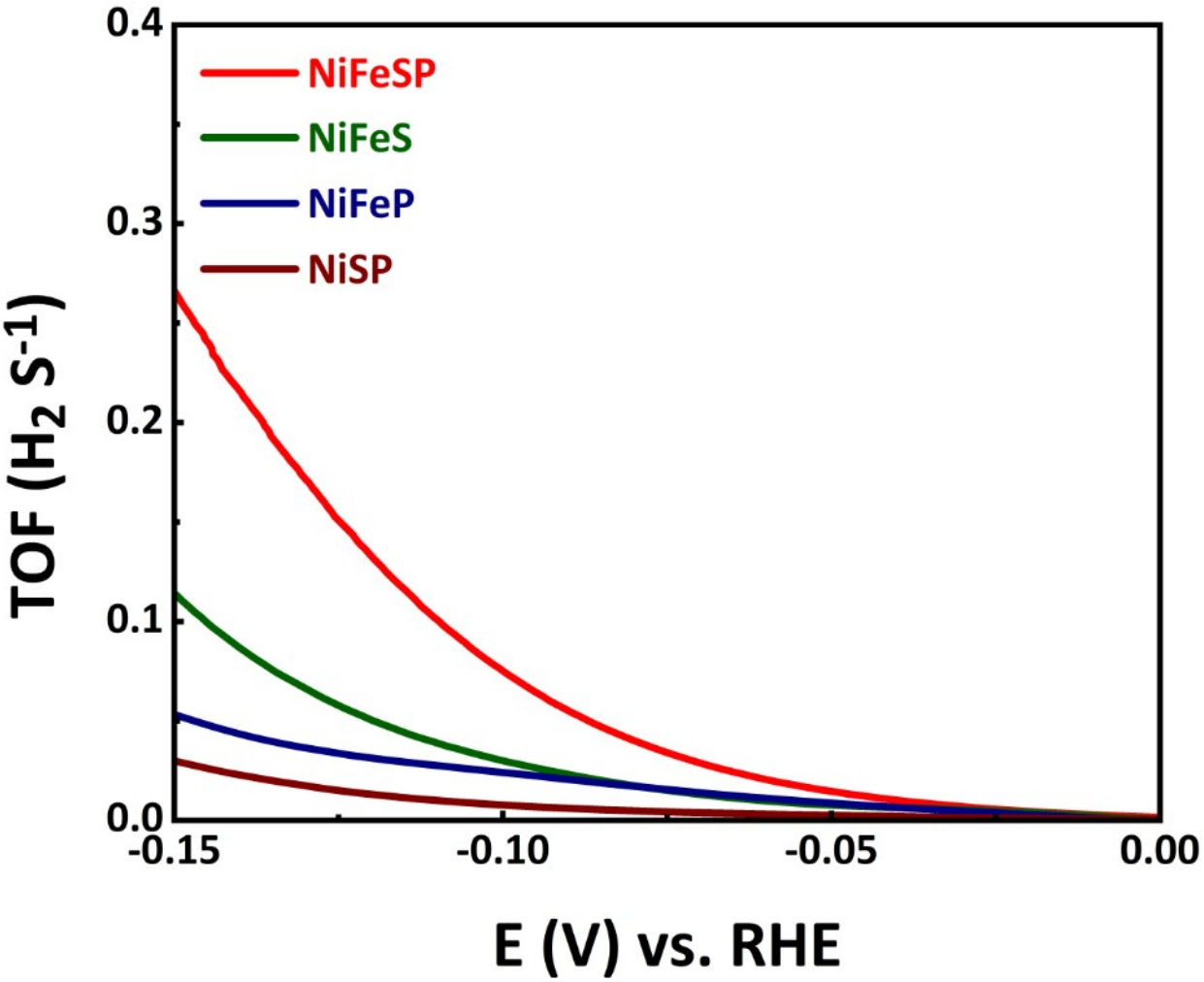

Figure S9 TOF plots for NiFeSP, NiFeS, NiFeP, and NiSP electrocatalyst.

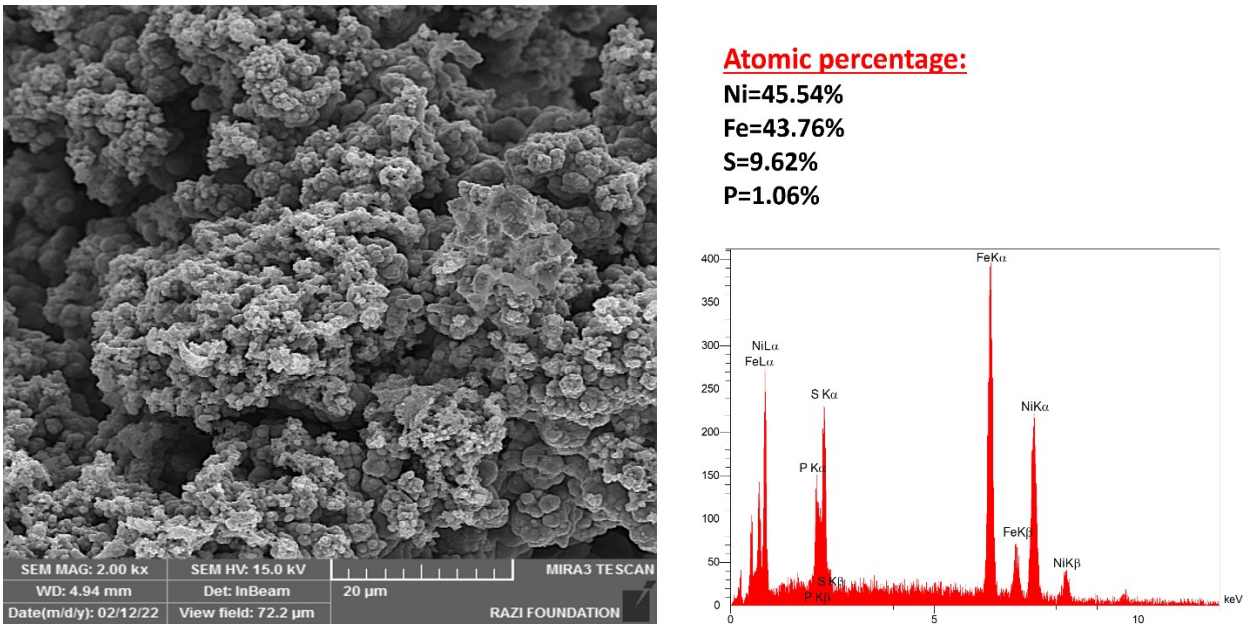

Figure S10 The FESEM image and EDS spectra of NiFeSP electrocatalyst after HER stability.

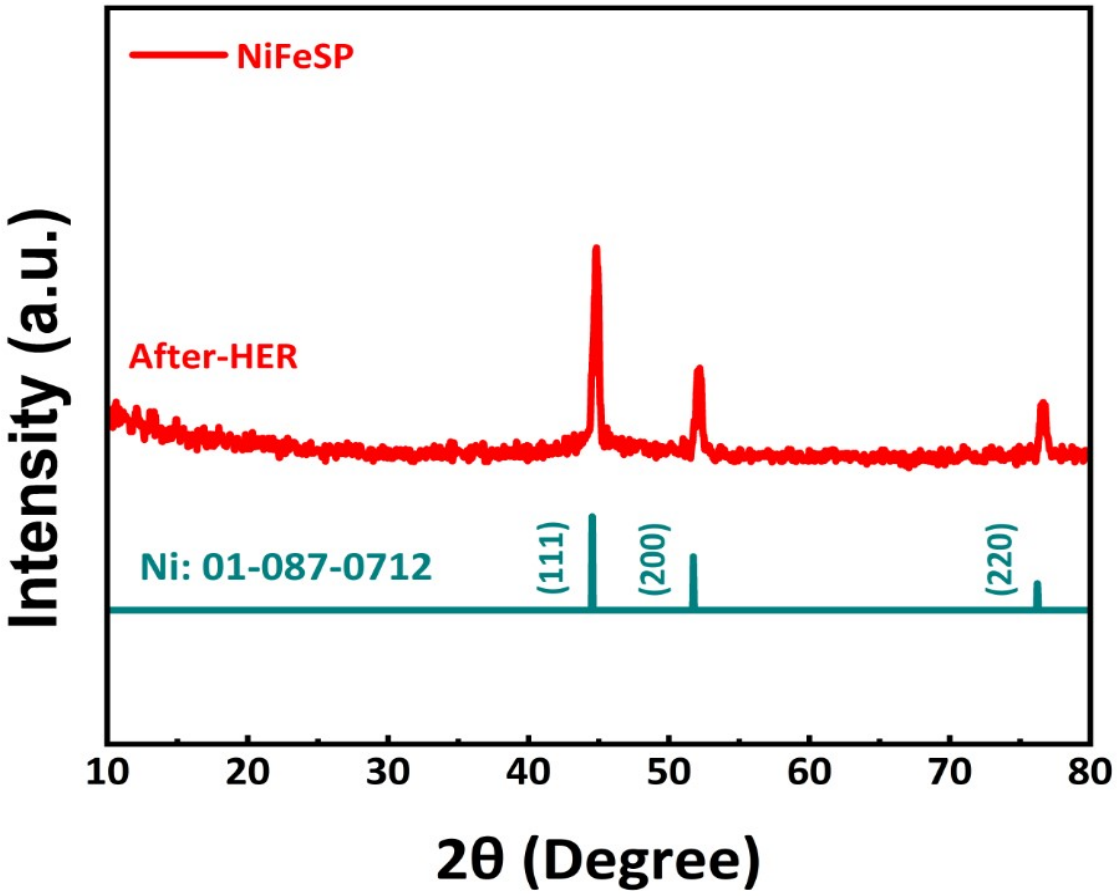

Figure S11 XRD pattern of NiFeSP/NF the after-HER.

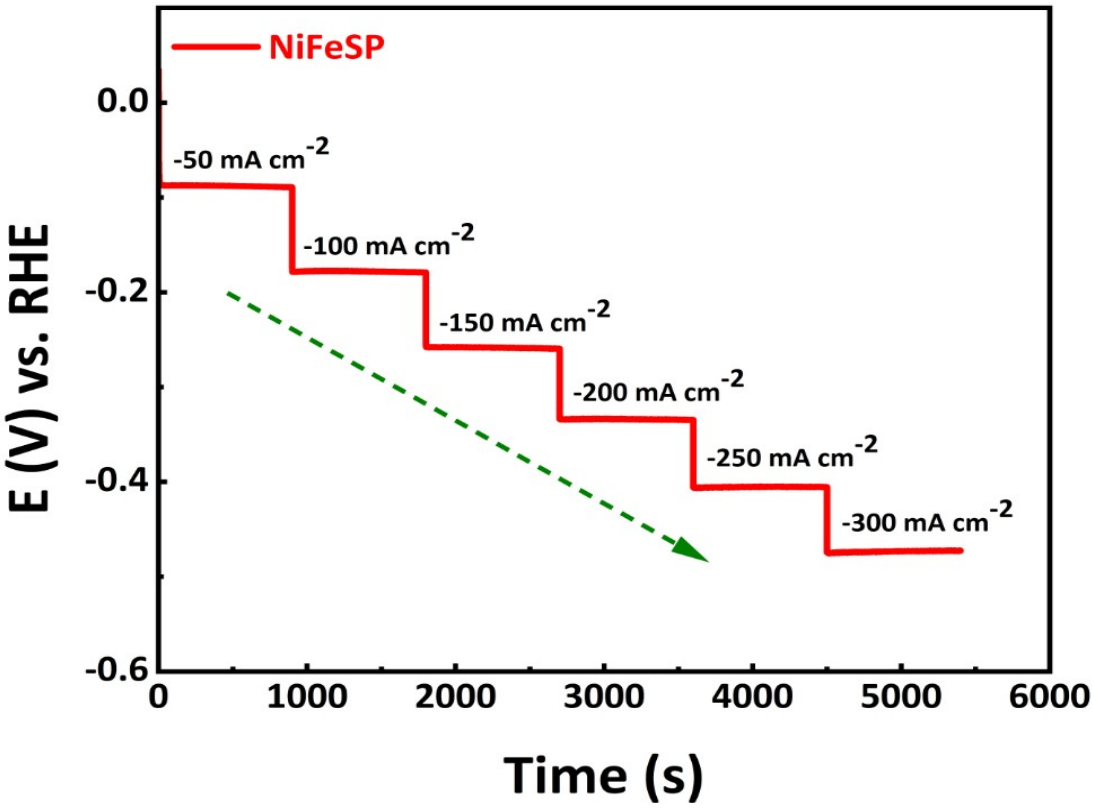

Figure S12 Multi-step chronopotentiometry of NiFeSP electrocatalyst in 1000.0 mM KOH.

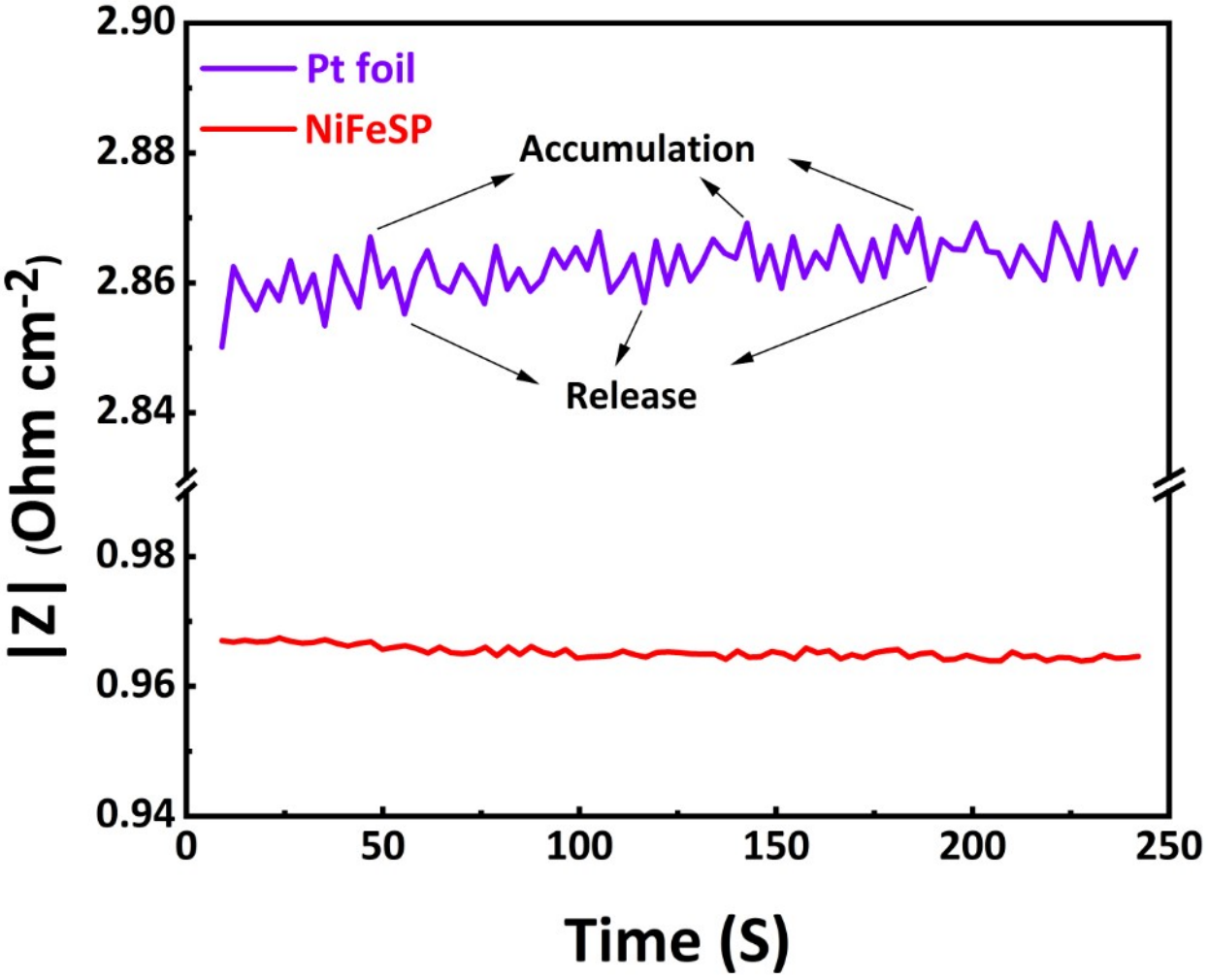

Figure S13 Operando dynamic specific resistance at an HER overpotential of -400 mV in 1000.0 mM KOH.

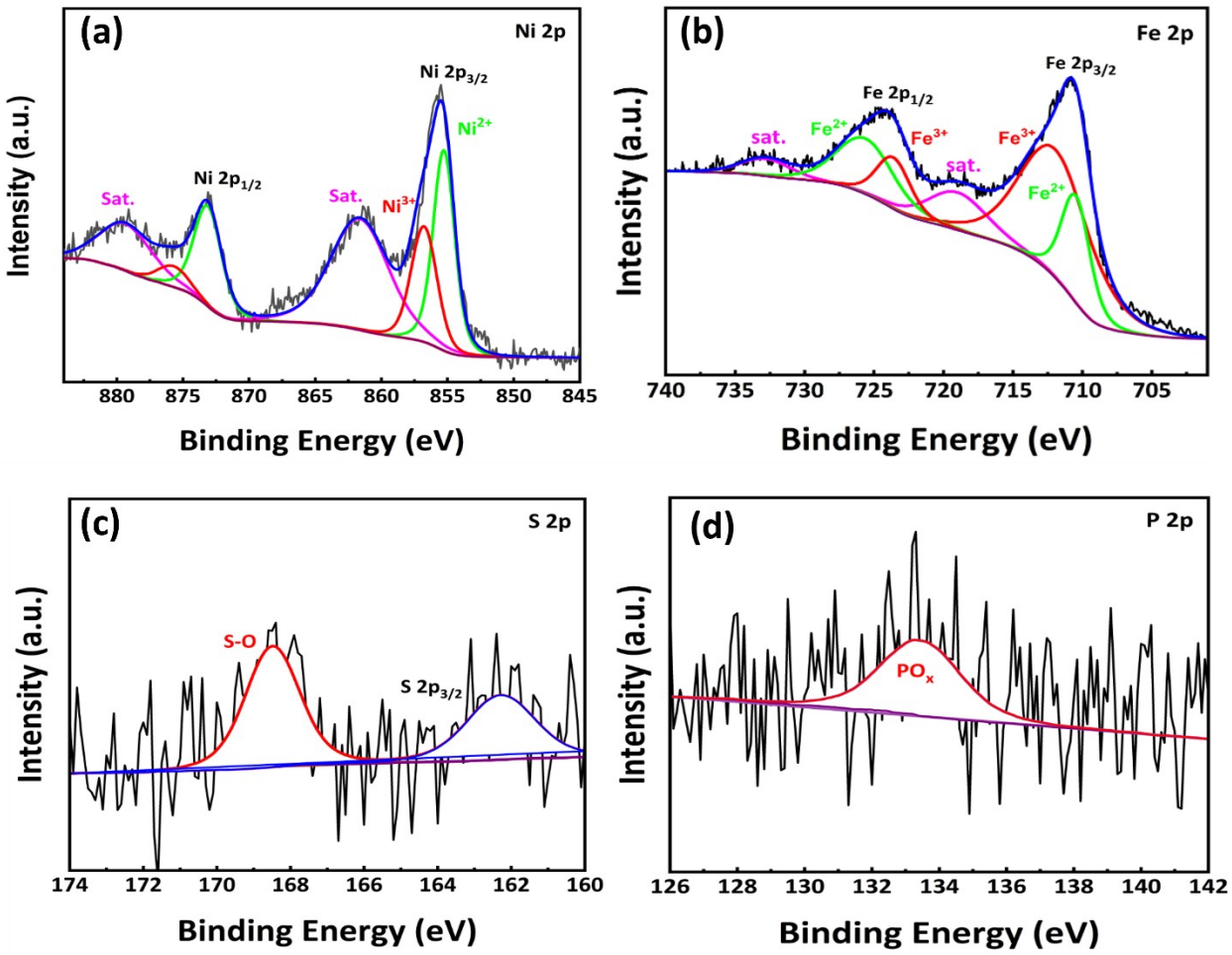

Figure S14 Ni 2p, Fe 2p, S 2p, and P 2p core level XPS spectra of NiFeSP nanostructure after stability in 1000.0 mM KOH + 330.0 mM urea solution.

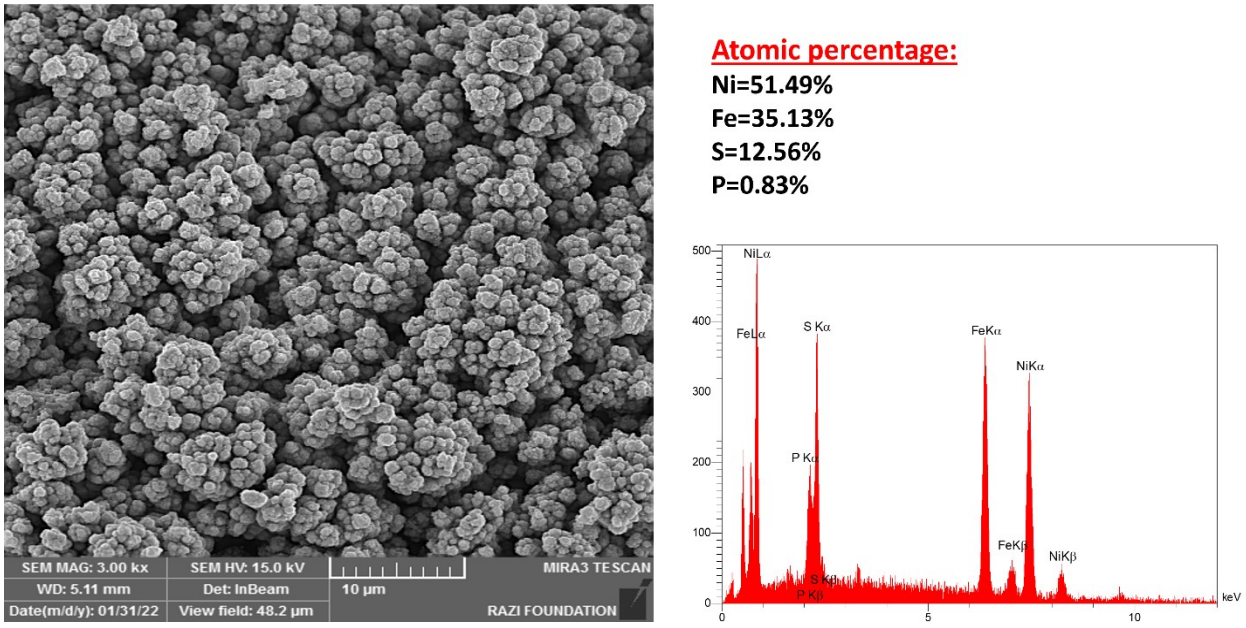

Figure S15 The FESEM image and EDS spectra of NiFeSP electrocatalyst after UOR stability.

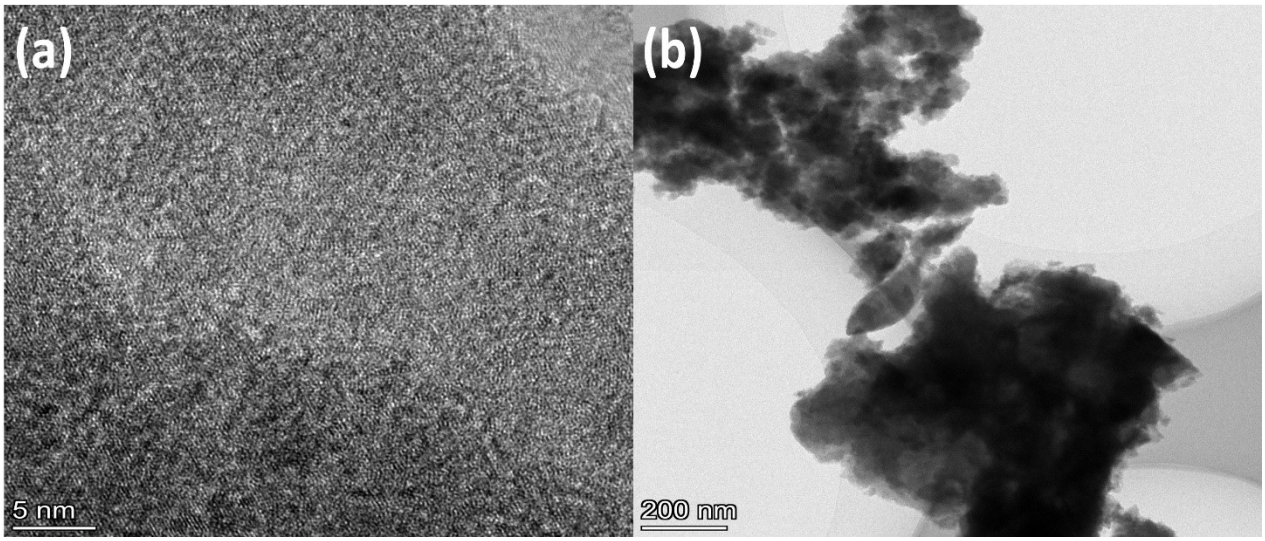

Figure S16 The TEM image and of NiFeSP electrocatalyst after UOR stability.

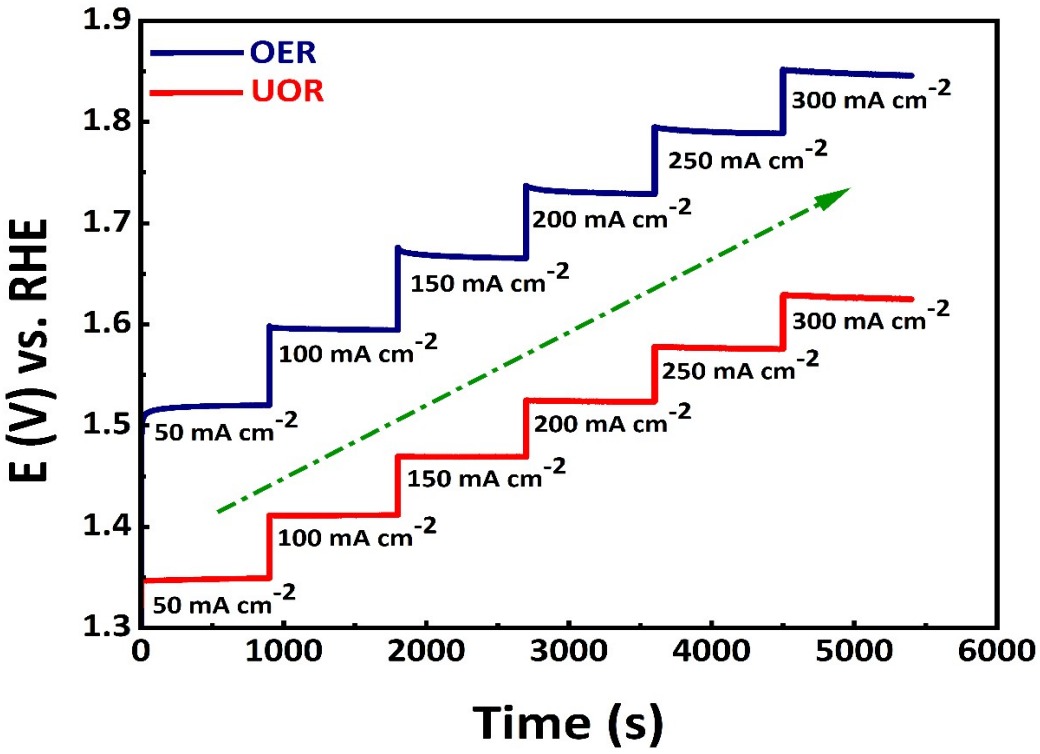

Figure S17 Multi-step chronopotentiometry of NiFeSP electrocatalyst in 1000.0 mM KOH (OER) and 1000.0 mM KOH + 330.0 mM urea (UOR).

Table S1 Comparison of catalytic parameters of NiFeSP and other non-noble metal electrocatalysts.

Catalyst	Electrolyte	Cell voltage at the corresponding j (V \\ mA.cm^{-2})	Reference
NiFeSP	1000.0 mM KOH + 330.0 mM urea	1.35 \\ 10 1.52 \\ 100	This work
$NiCo_2S_4$	1000.0 mM KOH + 330.0 mM urea	1.45 \\ 10	[1]
Fe doped-NiS-NiS_2	1000.0 mM KOH + 330.0 mM urea	1.55 \\ 10	[2]
N-$CoMoO_4$/P-$CoMoO_4$	1000.0 mM KOH + 500.0 mM urea	1.39 \\ 10	[3]
NP-$Ni_{0.70}Fe_{0.30}$	1000.0 mM KOH + 330.0 mM urea	1.55 \\ 10	[4]
CoNiOP	1000.0 mM KOH + 330.0 mM urea	1.42 \\ 50	[5]
$(NiFeCu)_3S_2$@(NiFeCu)O	1000.0 mM KOH + 330.0 mM urea	1.47 \\ 10	[6]
P-$CoNi_2S_4$	1000.0 mM KOH + 500.0 mM urea	1.40 \\ 10	[7]
NiFe NSs	1000.0 mM KOH + 330.0 mM urea	1.40 \\ 10	[8]
Fe–Ni_3S_2	1000.0 mM KOH + 330.0 mM urea	1.46 \\ 10	[9]
Mo/Ni-P	1000.0 mM KOH + 500.0 mM urea	1.42 \\ 10	[10]
CoP-Ni_2P	1000.0 mM KOH + 1000.0 mM urea	1.39 \\ 10	[11]
c-CoNiPx/a-P-MnOy	1000.0 mM KOH + 500.0 mM urea	1.60 \\ 50	[12]

Reference

1 W. Song, M. Xu, X. Teng, Y. Niu, S. Gong, X. Liu, X. He and Z. Chen, *Nanoscale*, 2021, **13**, 1680–1688.

2 S. Huang, Q. Zhang, P. Xin, J. Zhang, Q. Chen, J. Fu, Z. Jin, Q. Wang and Z. Hu, *Small*, 2022, **18**, 2106841.

3 Y. Guo, X. Liu, Y. Li, F. Ma, Q. Zhang, Z. Wang, Y. Liu, Z. Zheng, H. Cheng, B. Huang, Y. Dai and P. Wang, *Int J Hydrogen Energy*, 2022, **47**, 33167–33176.

4 Z. Cao, T. Zhou, X. Ma, Y. Shen, Q. Deng, W. Zhang and Y. Zhao, *ACS Sustain Chem Eng*, 2020, **8**, 11007–11015.

5 L. Yang and L. Zhang, *J Colloid Interface Sci*, 2022, **607**, 546–555.

6 F. N. Indah Sari, S. Marsaor Sihotang, S. Y. Li, Y. H. Shen and J. M. Ting, *ACS Sustain Chem Eng*, , DOI:10.1021/ACSSUSCHEMENG.2C06849/SUPPL_FILE/SC2C06849_SI_001.PDF.

7 X. F. Lu, S. L. Zhang, W. L. Sim, S. Gao and X. W. (David) Lou, *Angew Chemie*, 2021, **133**, 23067–23073.

8 Y. Diao, Y. Liu, G. Hu, Y. Zhao, Y. Qian, H. Wang, Y. Shi and Z. Li, *Biosens Bioelectron*, 2022, **211**, 114380.

9 J. S. Samdani, J. Sanetuntikul and S. Shanmugam, *Int J Hydrogen Energy*, 2022, **47**, 27347–27357.

10 L. Jiang, Y. Pan, J. Zhang, X. Chen, X. Ye, Z. Li, C. Li and Q. Sun, *J Colloid Interface Sci*, 2022, **622**, 192–201.

11 K. Wu, Y. Niu, N. Liu, C. Lyu, H. Li, P. Hu, X. Zhu, B. Jia, W. M. Lau and J. Zheng, *Catal Today*, , DOI:10.1016/J.CATTOD.2022.07.020.

12 L. Qiao, A. Zhu, D. Liu, J. Feng, Y. Chen, M. Chen, P. Zhou, L. Yin, R. Wu, K. W. Ng and H. Pan, *Chem Eng J*, 2023, **454**, 140380.